Palestinian Medical and Pharmaceutical Journal

Towards Improved Ulcerative Colitis Therapy: Utilizing a Colon-Activated Mutual Azo Prodrug of Procaine and Doxycycline

Rafid M. Hashim[1,*], Noor Waleed Ibrahim[2] & Monther Faisal Mahdi[2]

Type: Full Article. Received: 15th Sep. 2025, Accepted: 27th Nov. 2025, Published: ××××, DOI: https://doi.org/10.xxxx

Accepted Manuscript, In Press

Abstract: An innovative azo mutual prodrug combining procaine and doxycycline intended for colon-specific targeting was successfully synthesised and characterised. This study presents the synthesis and assessment of a new mutual azo prodrug (dox-proc) including doxycycline (antibacterial, anti-inflammatory) and procaine (to mitigate hyperactive autonomic nerves and uncontrolled immunological responses), specifically designed to target ulcerative colitis in the colon. In silico ADME profiling indicated unfavorable physicochemical properties for intestinal absorption, attributable to the compound's high molecular weight, hydrophilic log P, and elevated topological polar surface area (TPSA). Molecular docking studies revealed high binding affinity to azoreductase, with a docking score superior to that of sulfasalazine, suggesting efficient colonic bioactivation. Dox-proc was synthesized with a good yield (75 %) and purity (m.p: 258–260°C); The structure was validated by FTIR and ^{1}H-NMR spectroscopy. Pharmacokinetic study demonstrated low intestinal absorption potential (experimental log P = –1.65), dox-proc is high stabile in acidic/basic conditions. Fecal hydrolysis studies verified efficient enzymatic activation in the presence of azoreductase, with hydrolysis up to 81%. Biological studies show that dox-proc group had the lowest score (1.2 ± 0.310) in clinical activity score system, this indicated that dox-proc has the highest clinical activity. Histopathological study confirms a good sign of mucosal healing. These findings align with the in silico predictions and validate the compound's applicability as a colon-targeted therapy.

Keywords: Mutual azo prodrug; microbiota; Ulcerative colitis; Doxycycline; Procaine; Azoreductase.

Introduction

The two most prevalent forms of inflammatory bowel disease (IBD), which leads to persistent inflammation of the gastrointestinal tract, are ulcerative colitis (UC) and Crohn's disease. While the precise reason for inflammatory bowel disease is yet unclear, a prevailing hypothesis attributes its pathogenesis to an exaggerated host immune response against antigens derived from dietary components and/or the gut microbiota [1]. A contributing element has also been identified as an imbalance in the gut's autonomic nervous system innervation, with adrenergic dominance possibly causing intestinal mucosal damage through vasoconstriction and faster epithelium turnover [2, 3].

Chronic inflammation is recognized as a contributing factor in the advancement of some cancer forms. including colitis associated with colon cancer CAC [4], gastric cancer [5], and liver cancer [6]. Persistent inflammation can lead to the accumulation of mutations and epigenetic alterations within tissues, ultimately contributing to the development of malignancies [7-15]. Particularly in the colon, chronic inflammation and the resultant tumorigenesis are significantly influenced by the intestinal microbiota [16]. Studies have shown that antibiotic-mediated suppression of the microbiota can inhibit tumor development by reducing colonic inflammation [17-22]. The observed decrease in tumor incidence under germ-free conditions or following antibiotic treatment highlights the potentially large impact of targeting the microbiota for cancer prevention [23, 24]. This protective effect is thought to be mediated by a reduction in mutation frequency or levels of aberrant DNA methylation [25].

To mitigate systemic absorption and enhance localized delivery to the colon, a prodrug approach can be employed [26]. The synthesis of non-absorbable azo compounds, achieved by increasing hydrophilicity, yields site-specific prodrugs that undergo hydrolysis primarily within the colon. The colonic environment, rich in azoreductase enzymes, facilitates the breakdown of the azo bond, releasing the active drug constituents directly at the site of inflammation and dysbiosis [27].

In line with the understanding of the inflammatory and microbial contributions to UC and CAC, therapeutic strategies targeting these pathways are of significant interest [28].

Specifically, the conjugation of procaine with doxycycline to produce a non-absorbable azo prodrug offers a promising strategy. Within the colon, this prodrug can be hydrolyzed by azoreductase, releasing both procaine and doxycycline. This combined delivery has the potential to exert synergistic or additive therapeutic effects [29].

Procaine and doxycycline are two pharmacologically distinct agents with established roles in clinical medicine. Procaine is a local anesthetic of the ester class, commonly used to induce regional analgesia in minor surgical, dental, and obstetric procedures. It exerts its effect by blocking sodium channels, thereby inhibiting nerve signal transmission [30]. Major side effects of procaine include allergic reactions (due to its ester

1 Department of Pharmaceutical Chemistry, College of Pharmacy, Uruk University, Baghdad, Iraq.
* Corresponding author email: dr.rafedmohammad@uruk.edu.iq
2 Department of Pharmaceutical Chemistry, College of Pharmacy, Mustansiriyah University, Baghdad-Iraq. noorwaleed@uomustansiriyah.edu.iq
2 Department of Pharmaceutical Chemistry, College of Pharmacy, Mustansiriyah University, Baghdad-Iraq. dr.monther.f71@uomustansiriyah.edu.iq

structure), central nervous system stimulation or depression, and, rarely, cardiovascular complications such as hypotension or arrhythmia [31]. Although procaine is seldom used systemically, it has anti-inflammatory and membrane-stabilizing characteristics can help attenuate pain and promote mucosal healing have attracted interest for experimental approaches targeting inflammatory disorders. Procaine is thought to provide potential advantages by potentially calming overactive autonomic nerves and the uncontrolled immunological response [32].Doxycycline is a broad-spectrum tetracycline antibiotic widely prescribed for the treatment of bacterial disease [33]. It inhibits bacterial protein synthesis by attaching to the 30S ribosomal subunit. its major adverse effects include gastrointestinal discomfort, photosensitivity, esophageal irritation, and, on rare occasions, hepatotoxicity or hypersensitivity reactions. Doxycycline can directly target the gut flora and help to reduce inflammation [34], including inhibition of metalloproteinases and modulation of neutrophil activity. By minimizing systemic exposure and related adverse effects, localized delivery may improve both medications' therapeutic index and lower the risk of CAC linked to persistent colonic inflammation [35].

The purpose of this research is to develop, synthesize, and analyze dox-proc, a new mutual azo prodrug, for the targeted therapy of ulcerative colitis in the colon. This includes in silico, in vitro, and in vivo evaluation of the prodrug's pharmacokinetic properties, stability, enzymatic activation, and therapeutic efficacy, with the goal of achieving site-specific drug release and enhanced healing of colonic tissue by reduce colonic inflammation, restore microbial balance, and improve outcomes in UC individuals beyond those achievable with conventional-therapies.

Experimental Procedures

Chemistry

Reagents and Materials

All the solvents and reagents were of the type reagent-grade.

Instrumentation

Infrared spectra were recorded using the Shimadzu FT.IR. IR Affinity-1S (in KBr pellets). A melting point device (Stuart SMP20) was used to measure melting points and UV spectra were documented using a shimadzu UV/V Spectrophotometer (UV-1800). Thin layer chromatography of dox-proc compound was conducted on precoated silica gel 60 F264 plates (Merck) using the specified solvent system: n -Butanol: Acetic Acid: Water (4:1:1), using iodine fumes and ultraviolet light for visibility. The nuclear magnetic resonance (NMR) examinations were carried out at the facilities of Al Al-bayt University in Jordan using a Bruker Ultra Shield 300 MHz spectrophotometer.

Chemical synthesis

The azo prodrug was synthesized by dissolving 1.36 g (0.005 moles) of procaine HCl in 1.2 mL of Conc. HCl (37% w/w), adjusting the total volume to 10 mL with D.W, and subsequently adding a dropwise solution of 0.345 g (0.005 mole) of sodium nitrite in 10 mL of D.W to produce the salt of diazonium at a temperature below 5 °C.

Add an alkaline solution containing (2.2 g, 0.005 moles) of doxycycline in 1.2 percent w/v NaOH to the diazonium solution. The flask's contents were meticulously agitated. A rich orange coloring was noted; A rotary evaporator was used to evaporated the solvent followed by an oven drying. The prodrug was purified by recrystallization from methanol [36,37]. Yield: 75 %; m.p: 258–260°C

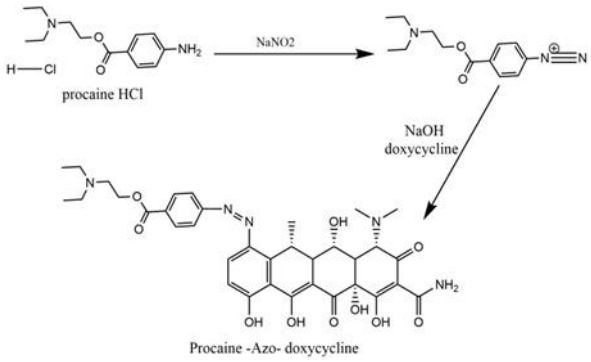

Scheme (1): Synthesis of dox-proc -azo compound.

COMPUTATIONAL METHODS

ADME procedures

Swiss ADME, a free online tool for assessing ADME characteristics and small molecules drug-likeness, was employed to forecast the ADME characteristics and drug like properties of produced compound. Lipinski's five rules, which states that chemical that fails to meet more than two of these standards (polar surface area (PSA) less than 140 Å2, molecular weight less than 500, sum of Hydrogen-bond donors equal or less than 5, sum of Hydrogen-bond acceptors equal or less than 10, and computed log p fewer than 5) is considered poorly

absorbed or impermeable, This is critical throughout the drug's preclinical phase of development. [38, 39]. Final ligand is drawn using ChemBioOffice (v. 22.0.0.22), and the Swiss ADME tool, which forecasts the pharmacokinetic parameters and physicochemical descriptors, converts them to SMILE names [40].

Molecular docking

Molecular docking is extensively employed to explore potential binding conformations of chemical compounds within a receptor [41]. This study aimed to investigate the interactions between the mutual prodrug dox-proc and the active site residues of the azo reductase enzyme. It also sought to compare binding affinities and RMSD values between dox-proc and sulfasalazine, as well as to identify the optimal conformers based on the highest binding affinities. Molecular docking of the identified enzyme and dox-proc was performed using Molecular Operating Environment (MOE) software version 2024.06 [42]. The crystal structure of YhdA-type Azoreductase from Bacillus velezensis (PDB ID: 7BX9) is illustrated in Figure 1, while the experimental data, including a resolution of 1.38 Å, is presented in Table 1. This data was obtained from the RCSB database. (http://www.rcsb.org/pdb).

which is in the bound state with co-crystallized ligand Flavin mononucleotide (FMN) (Figure 2). The docking procedure has two stages:

First: Preparing the ligand

Energy minimization and conformational analysis of molecules (level: ultra) using Chem3D Pro 19.1 software have been performed on all previously drawn molecular structures of dox-proc, sulfasalazine and FMN. using the Molecular Mechanics Force Field (MM+), such as MM2 and MMFF94. Until the root mean square (RMS) gradient value drops below 0.1 kcal/mol, this procedure is repeated. The ligand is then protonated in three dimensions in MOE, followed by partial charge addition, energy minimization, and ultimately results saving [43].

Secondly: the preparation of proteins

The crystal structure of the X-ray structure of YhdA-type azoreductase from Bacillus velezensis (PDB ID: 7BX9) was prepared using the following steps:

Only the chain sequences involved in the protein action were selected. The small molecules and superfluous water molecules were eliminated. Incorporating hydrogen conceals bonds; subsequently, stabilizes the potential of the protein atoms and determine its active sites [44]. Ultimately, all previously prepared ligands—dox-proc, sulfasalazine—are imported into MOE from saved data, followed by the docking process with the co-crystallized ligand FMN for validation of the docking protocol. Poses exhibiting higher binding affinity, indicated by lower S scores, and appropriate RMSD values were selected. Table 3 presents the binding affinity, RMSD value, interaction type, bond distance (Å), and bonding energy E (kcal/mol) between the ligands and the atoms of the involved residues at the active site of the 7BX9 protein [45].

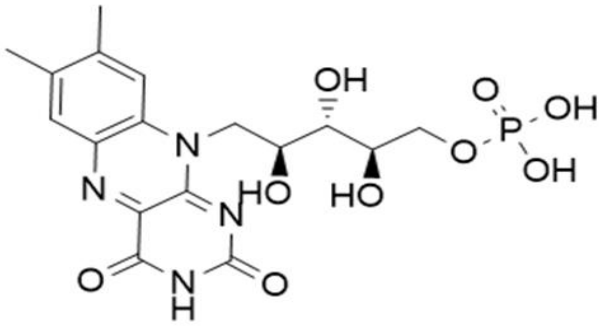

Figure (1): The X-ray crystallographic structure of Azoreductase derived from Bacillus velezensis (PDB ID: 7BX9).

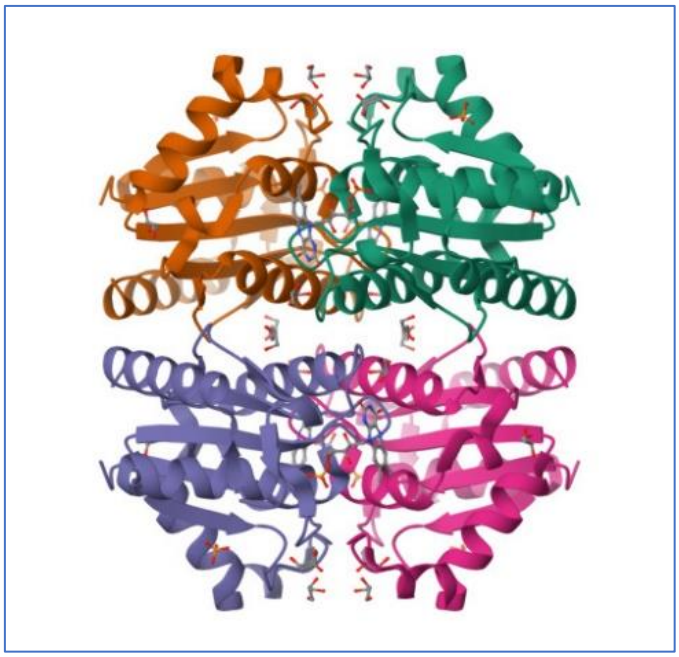

Figure (2): Molecular structures of co-crystallized ligand (FMN).

Table (1): Information details of Azoreductase enzyme (PDB ID: 7BX9).

protein	Method	Resolution (Å)	Amino acid number	Atom Count	Total Structure Weight	Organism	Co-crystalized ligand	Docking Score	RMSD
7BX9	X-ray diffraction	1.38	168	1,608	19.64 kDa	Bacillus amyloliquefaciens	Flavin mononucleotide (FMN)	-6.15	1.52

In vitro kinetic evaluation

To ensure targeted delivery of the mutual azo prodrug (dox-proc) to the colon, it is essential to evaluate its absorption profile in the upper gastrointestinal tract. This can be predicted by measuring the partition coefficient (log P) of the prodrug [46]. Additionally, stability assessment of the prodrug in simulating gastric and intestinal fluids determines its resistance to premature degradation. Finally, colon-specific activation is confirmed by investigating hydrolysis of the prodrug by bacterial azoreductase, resulting in the release of active constituents (doxycycline and procaine) specifically in the colon [47].

Partition Coefficient

The partition coefficients of the synthesized mutual prodrug dox-proc were determined in n-octanol/phosphate buffer (pH 7.4) at room temperature (25 ± 10 ˚C). Dox-proc, a prodrug, was individually dissolved in 10 mL of n-octanol and 10 mL of phosphate buffer [47]. The two solutions were gradually combined, and the octanol-phosphate buffer mixture was agitated on a wrist shaker for 48 hours to achieve distribution equilibrium. The volumes of each phase were selected to facilitate the determination of solute concentrations using a UV spectrophotometer for the calculation of the partition coefficient.

Solubility in water

The aqueous solubility of dox-proc was determined at room temperature (25 ± 10˚C). Excess amount of the dox-proc was added to D.W in stoppered conical flask then sonication is conducted finally the mixture was stirred for 24 h. It was ensured that saturation equilibrium was established. Filtration was done then Absorbance was determined on UV-spectrophotometer to be applied on calibration curve of dox-proc [48, 49].

Release study of dox-proc in acidic and basic buffer and in fecal material

The kinetics of the synthesized prodrug dox-proc were

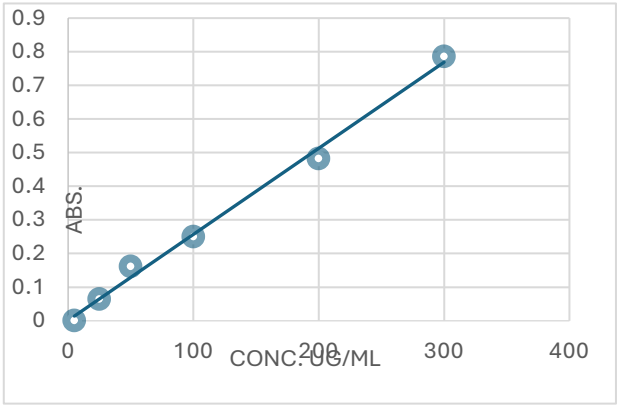

examined at 37°C in aqueous buffer solutions with pH levels of 1.2 and 7.4. The overall buffer concentration was typically 0.05 M. The reaction was monitored using UV spectroscopy, and the concentration was determined from the dox-proc calibration curve (Fig. 3). The decrease in the concentration of the prodrug was recorded over time. The hydrolysis percentage of dox-proc in the presence of rat fecal material, which contains the azo reductase enzyme, was determined using the previous data. The kinetic studies were conducted in triplicate [50].

Release analysis in 0.05 M phosphate buffer (pH 7.4) and 0.05 M hydrochloric acid buffer (pH 1.2)

The synthesized prodrug dox-proc (10 mg) was introduced into 900 mL of HCl buffer contained in a basket and maintained at a constant temperature of 37 °C. The solution was stirred intermittently, and 5 mL aliquots were extracted at different time intervals. When the spectrum of active constituents (doxycycline, procaine) and prodrug overlapped, it was observed that the dox-proc did not interfere in the absorption range of active constituents, as is obvious from the difference in the λ max values of procaine (219 nm), doxycycline (271 nm) and its prodrug (257 nm).

The aliquots were directly measured using a UV spectrophotometer at 257 nm to determine the concentration of the remaining prodrug. The procedure outlined previously was executed with the substitution of phosphate buffer for the HCl buffer. The kinetics were assessed through the temporal reduction in prodrug concentration.

Release test in rat fecal material (pH 7.4)

The dox-proc was dissolved in phosphate buffer at pH 7.4, resulting in a final concentration of 300 µg/mL. Approximately 1 g of fresh rat fecal material was weighed and distributed into various test tubes. Each test tube received 1 mL of dox-proc solution, which was then diluted to a final volume of 5 mL using phosphate buffer to reach a concentration of 60 µg/mL. The test tubes were incubated at 37 ˚C. The concentration of dox-proc was measured using a double beam UV-spectrophotometer at 257 nm at 15-minute intervals. The concentration of the residual prodrug was ascertained using the calibration curve of dox-proc (Fig. 3).

Figure (3): Calibration curve of dox-proc prodrug.

Animal study

Thirty-six adult male albino-Wister rats, weighed 200-250g and aged four to six months, were obtained from the animal shelter of the Iraqi Center for Cancer and Medical Genetics Research. The rodents were confined in cages with wire mesh bottomed and tops enclosure. For the duration of the investigations, the rodents are permitted to have unrestricted access to water and laboratory chow (LabDiet 5001), and the temperature is maintained at 23 ± 1 ˚C with a 12 h light/dark cycle [51]. The Animal Ethics Committee of the College of Pharmacy at Mustansiriyah University has approved the protocol and procedures outlined below.

Colitis Induction

Acetic acid is utilized to induce ulcerative colitis; a colonic lesion was created by administering a single intra-colonic dose of 2 mL of (4% v/v) acetic acid (AA) through a pediatric catheter (size 6 F) following a 24-hour fasting period [52]. The catheter was inserted into the rectum to a depth of 8 cm [53]. To prevent anal leakage, the animals were positioned vertically with their heads directed downward for a duration of 2-3 minutes. The control group of rats received identical treatment with an equivalent volume of normal saline substituting for AA. The rats were housed for three days with unrestricted access to food and water, but not subjected to treatment, to facilitate the development of a complete ulcerative colitis model [54].

Experimental design

The rats were split into six equal groups at random, with six individuals in each group (n=6).

Group I: Normal Control (apparently healthy): were received normal saline (2mL) intrarectally with no other treatment.

Group II: induction (AA) group: served as a colitis induction group, were received only 4% v/v AA (2mL) intrarectally.

Group III: dox-proc treatment group, received 4% v/v AA (2mL) intrarectally + dox-proc as a standard therapy (100 mg /kg) orally once/day for 8 days.

Group IV: SULF treatment group, received 4% v/v AA (2mL) intrarectally + SULF as a standard therapy (100 mg /kg) orally once/day for 8 days.

Group V: doxycycline treatment group, were received 4% v/v AA (2mL) intrarectally + doxycycline as a standard therapy (65 mg /kg) orally once/day for 8 days.

Group VI: procaine treatment group, were received 4% v/v AA (2mL) intrarectally + procaine as a standard therapy (35 mg /kg) by oral once per day for 8 days [55].

For eight days, dox-proc was given orally by gavage. Rats were put to death on day 8 of the experiment by breathing too much diethyl ether following a 24-hour fast. The abdomen was then promptly dissected and opened, and the colon was extracted [51,56.57].

Assessment of colitis treatment

Clinical activity scoring system

All rats' colitis activities were measured using a clinical activity score measuring weight loss, stool consistency, and rectal bleeding over 12 days. Clinical activity score was calculated by averaging the aforementioned three criteria for each day, for each group, and ranging from 0 (healthy) to 4 (maximal colitis activity).

Histological evaluation

Colon samples were washed with cold saline. Colon samples were somewhat extended. After fixing the colon samples in 10% formaldehyde, gradient ethanol dehydration, paraffin embedding, and sectioning followed. Next, 5-µm slices were put on slides, followed by cleaning, hydration, and H&E staining. Specialized pathologists screened and assessed without seeing or knowing the groups. Every specimen of tissue on a slide was examined using a 100X light microscope. Each tiny region was scored. Damage features were examined which, including sub-mucosal oedema, damage/necrosis, vasculitis, inflammatory cell infiltration, perforation, complete crypt loss, and intestinal damage [52].

Results And Discussions

FT-IR results

FT-IR ((KBr)), vmax (cm−1): 3600-3100 cm-1 v (O-H & N-H broad), 1708 cm-1 v (C=O, ester), 1643 cm-1 v (C=O, ketone & amide), 1598 cm-1 v (C=C), 1448cm-1 v (N=N, azo), 1386cm-1 v (C-N).

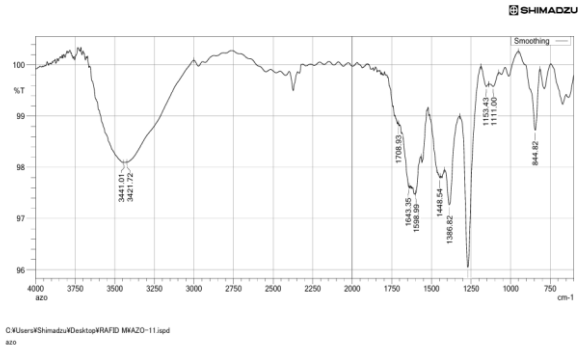

Figure (4): FT-IR spectrum for Azo Prodrug of dox-proc.

1H-NMR results

1H NMR (300 MHz, DMSO-d6) δ =7.81 (d, J = 13.6 Hz, 1H), 7.73 (d, J = 7.0 Hz, 3H), 7.34 (s, 1H), 7.30 (s, 1H), 7.09 (d, J = 13.6 Hz, 2H), 6.70 (d, J = 12.8 Hz, 1H), 4.15 (s, 1H), 3.71 (s, 2H), 3.14 (s, 4H), 2.92 (s, 1H), 2.88 (s, 3H), 1.29 – 1.24 (m, 6H), 0.87 – 0.80 (m, 1H).

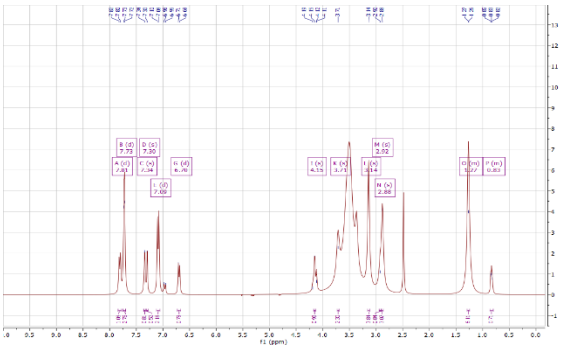

Figure (5): ^{1}H-NMR spectrum for Azo Prodrug of dox- proc.

Molecular docking results

All designed dox-proc and sulfasalazine were docked using Molecular Operating Environment (MOE) 2024.06 with the identified active site (56 residues) (Table 2) of 7BX9 protein along with FMN (co-crystallized ligand) for validation of the docking protocol.

(Table 3) presents the binding affinities (S scores) and RMSD values, alongside the types of interactions (Hydrogen-bonds, hydrophobic, metal coordination), bond distances (Å), and bonding energies (E in kcal/mol) between the atoms of all ligands and the atoms of the relevant residues within the identified active site of the (7BX9) receptor. Subsequently, the comparative performance was assessed against sulfasalazine (SULF). Examining binding affinities (S scores), interaction profiles, and structural stability (RMSD).

Table (2): Binding site residues of the X-ray structure of Bacillus velezensis azoreductase enz. (PDB ID: 7BX9).

Receptor	Size	Residues
7BX9	56	1:(THR9 ARG11 ASN13 GLY14 ARG15 THR16 PRO72 GLU73 TYR74 HIS75 SER76 ALA104 ALA105 GLY106 GLY110 GLY111 LEU136 ASP137 PRO138 MET143)

Table (3): docking results of ligands with the active site of azoreductase (7BX9).

Active site			Bonds between atoms of ligands and residues of the active site of 7BX9.					
Compound	S score (kcal/mol)	RMSD (Å)	Atom of compound	Involved receptor atoms	Involved receptor residues	Type of interaction	bond Distance (Å)	E (kcal/mol
Co-crystalized ligand (FMN)	-11.2396	1.623034	N3 4	OE1	GLU 73 (A)	H-donor	3.05	-4.1
			O2 3	N	GLY 106 (A)	H-acceptor	3.12	-3.5
			O2 3	O	HOH 329 (A)	H-acceptor	2.90	-1.2
			O4 7	N	SER 76 (A)	H-acceptor	3.24	-1.3
			O4 7	O	HOH 358 (A)	H-acceptor	2.91	-1.4
			N5 9	N	HIS 75 (A)	H-acceptor	3.10	-1.9
			O2' 33	NH2	ARG 11 (A)	H-acceptor	3.16	-1.8
			O2' 33	O	HOH 436 (A)	H-acceptor	3.02	-0.6
			O4' 41	NH1	ARG 15 (A)	H-acceptor	3.21	-0.6
			O5' 46	NH2	ARG 11 (A)	H-acceptor	3.14	-1.7
			O3P 48	N	THR 16 (A)	H-acceptor	2.91	-7.2
			O3P 48	OG1	THR 16 (A)	H-acceptor	2.80	-4.0
			O2P 49	OG1	THR 9 (A)	H-acceptor	2.84	-3.9
			O2P 49	NE	ARG 11 (A)	H-acceptor	3.28	-4.4
			O2P 49	NH2	ARG 11 (A)	H-acceptor	3.28	-3.5
			O2P 49	OH	TYR 74 (A)	H-acceptor	2.73	-4.7
			O1P 50	CA	GLY 14 (A)	H-acceptor	3.05	-0.7
			O1P 50	N	ARG 15 (A)	H-acceptor	3.29	-3.1

Active site			Bonds between atoms of ligands and residues of the active site of 7BX9.					
Compound	**S score (kcal/mol)**	**RMSD (Å)**	**Atom of compound**	**Involved receptor atoms**	**Involved receptor residues**	**Type of interaction**	**bond Distance (Å)**	**E (kcal/mol**
			O1P 50	O	HOH 353 (A)	H-acceptor	2.69	-3.5
			O2P 49	NE	ARG 11 (A)	Ionic	3.28	-2.9
			O2P 49	NH2	ARG 11 (A)	Ionic	3.28	-2.9
			O1P 50	NE	ARG 11 (A)	Ionic	3.41	-2.3
			O1P 50	NH2	ARG 11 (A)	Ionic	2.99	-4.5
			C6 11	5-ring HIS	75 (A)	H-pi	3.76	-0.6
			6-ring	6-ring TYR	74 (A)	pi-pi	4.37	
SULF	-8.41389	1.822368	N 8	N	HIS 75 (A)	H-acceptor	3.01	-0.5
			O 11	N	SER 76 (A)	H-acceptor	3.46	-1.0
			O 11	O	HOH 358 (A)	H-acceptor	3.01	-1.5
			O 27	CA	GLY 14 (A)	H-acceptor	3.32	-0.5
			O 27	N	ARG 15 (A)	H-acceptor	2.82	-3.2
			O 27	O	HOH 353 (A)	H-acceptor	2.68	-0.7
			O 29	OG1	THR 9 (A)	H-acceptor	2.87	-2.9
			O 29	NE	ARG 11 (A)	H-acceptor	3.19	-3.3
			O 29	NH2	ARG 11 (A)	H-acceptor	3.07	-6.6
			O 29	OH	TYR 74 (A)	H-acceptor	3.03	-3.3
			O 30	N	THR 16 (A)	H-acceptor	2.95	-6.8
			O 30	OG1	THR 16 (A)	H-acceptor	2.86	-1.9
			O 29	NE	ARG 11 (A)	Ionic	3.19	-3.3
			O 29	NH2	ARG 11 (A)	Ionic	3.07	-4.0
			6-ring	CA	TYR 74 (A)	pi-H	3.78	-0.7
dox-proc	-7.51271	1.426411	O 45	O	HOH 455 (A)	H-donor	2.95	-1.9
			O 47	O	GLU 73 (A)	H-donor	2.67	-1.4
			O 38	O	HOH 329 (A)	H-acceptor	3.07	-0.8
			O 40	O	HOH 436 (A)	H-acceptor	2.69	-0.8
			O 44	O	HOH 498 (A)	H-acceptor	2.79	-2.5
			O 49	N	HIS 75 (A)	H-acceptor	3.12	-3.8
			O 49	O	HOH 459 (A)	H-acceptor	2.93	-0.7
			O 45	O	HOH 455 (A)	H-donor	2.95	-1.9

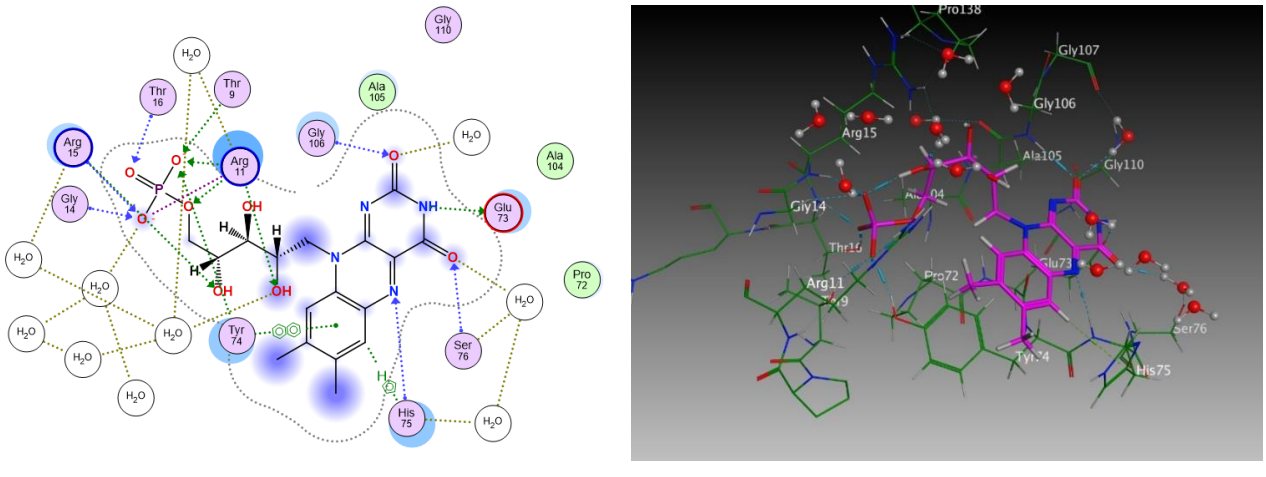

(A)FMN

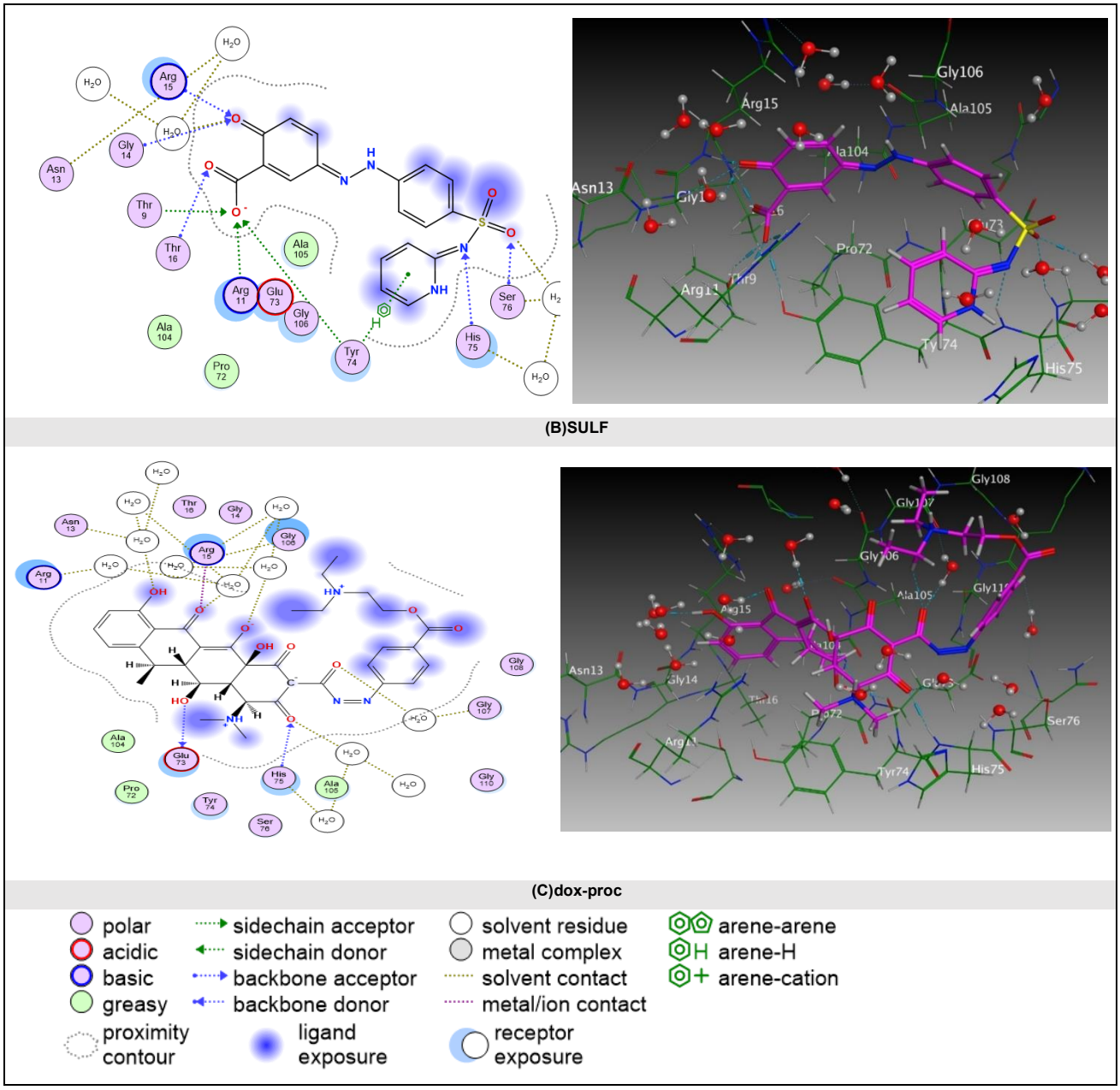

Figure (6): 3D (right) and 2D (left) visualization of the interactions between (A) FMN (B) SULF (C) dox-proc and the active site of the (7BX8) azoreductase enzyme.

Results of ADME Studies

Final manufactured substance pharmacokinetic characteristics: absorption, distribution, metabolism, excretion were assessed. A very helpful descriptor for estimating some ADME features, particularly the drug absorption, is topological polar surface area (TPSA), which was measured [58]. Therefore, it is believed that ligands with a TPSA >140 A^{o} have poor gastric permeation. Dox-proc result indicated that values of TPSA above 140, which is (235.88) so is typically associated with very low intestinal absorption because highly polar molecules struggle to cross the non-polar cell membranes of the small intestine. The most direct indicator, GI absorption, is listed as 'Low'. This is the primary parameter for assessing intestinal absorption and it directly confirms your design goal. Dox-proc has 3 violations of Lipinski's rule. (high molecular weight 676, Hydrogen-bond acceptor 14, Hydrogen-bond donor 6, TPSA >> 140 Å2) In which this important rule is a key principle designed for evaluating a drug's oral bioavailability. Having more than one violation is a strong indicator of poor oral absorption. The data shows the compound is a 'No' for BBB permeant, indicating it has poor ability to cross biological membranes as we see in table (4), which further supports the finding of low overall absorption. In summary, the combined results from the GI absorption, Lipinski's Rule of 5 violations, and TPSA all corroborate our design goal of creating a prodrug that is not absorbed by the small intestine [59].

Table (4): ADME properties summary of dox-proc prodrug.

Compound	Formula	M.Wt (g/mol)	H-bond acceptors	H-bond donors	TPSA	GI Abs.	BBB permeant	Lipiniski violations
Dox-proc	$C_{35}H_{41}N_5O_{10}$	691.73	14	6	235.88 Å^2	Low	No	3

Results of kinetic study

The water solubility of dox-proc was determined to be 0.45 g/mL. The log P value was determined to be -1.65, significantly lower than that of procaine (log P: 1.1) and doxycycline (log P: 0.02). The outcome of the aqueous solubility assessment of dox-proc aligns with the observed log P value. The higher

aqueous solubility of dox-proc would ensure that without getting absorbed in the upper GIT, it would pass intact into colon to deliver its active constituents there (through hydrolysis of prodrug by azoreductase enzyme). The kinetics of dox-proc in a 0.05 M hydrochloric acid buffer (pH 1.2) demonstrated a negligible release of procaine or doxycycline was noted, while in phosphate buffer (pH 7.4), a release of only 17% was observed over a duration of 6 hours.

The objective of bypassing the upper gastrointestinal tract without any free drug release was successfully achieved. The kinetics were further investigated in rat fecal material to validate the colonic reduction of the azo prodrug dox-proc. The release exhibited first-order kinetics, characterized by a t½ value of 95 minutes. During a duration of 6 hours, 81% of dox-proc prodrug is hydrolyzed, releasing doxycycline and procaine to the colon. The percentage of the hydrolyzed prodrug was calculated from above data and is depicted in Fig. 7.

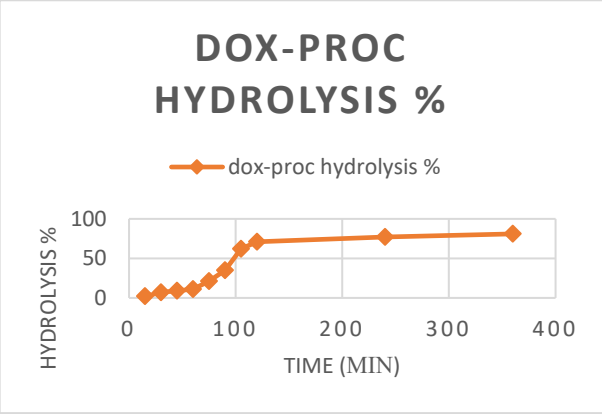

Figure (7): Hydrolysis of dox-proc prodrug in rat fecal material.

Biological results

Clinical activity score

Following the induction of colitis, the clinical activity score exhibited a rapid and consistent increase across all AA-treated groups over the subsequent three days (Fig. 8). Following a delay of 2 to 3 days, all groups receiving the treatments exhibited a differential reduction in inflammation severity. Following day 6, a notable disparity was observed between the groups receiving the treatments and the AA group. On the 12th day, the group receiving dox-proc exhibited the lowest score (1.2 ± 0.310), while the SULF group (1.4 ± 0.388), suggesting that dox-proc demonstrates the highest clinical activity. And when comparing these finding with result of doxycycline group (2.4 ± 0.410) and procaine group (2.4 ± 0.21) indicated that dox-proc prodrug enhanced the efficacy of doxycycline and procaine, and the effect was dose dependent.

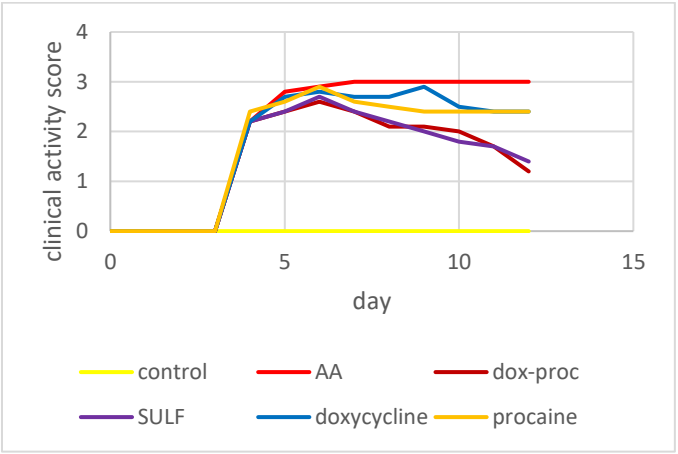

Figure (8): Clinical activity score during the whole experimental period.

Statistical analysis

The data were presented as mean ± standard error. The p-value was calculated as 0.05. The differences among groups were evaluated through one-way analysis of variance (ANOVA) and Tukey's post hoc test (SAS Institute: SAS 2002, User's Guide: Statistics). A p-value below 0.05 was considered significant in the results.

Histological evaluation

The severity of inflammation can be assessed through the direct detection of histological damage. The health control group exhibited normal mucosa, connective tissue, and muscularis (Fig. 9). Histopathological features in the AA group exhibited severe colitis, characterized by the absence of epithelial cells and significant mucosal/submucosal infiltration of inflammatory cells (Fig. 10). The dox-proc and SULF groups exhibited positive healing indicators, with the dox-proc group demonstrating superior corrected colon morphology compared to the SULF group (Fig. 11 and Fig. 12). Both doxycycline and procaine groups presented moderate mucosal abscess and inflammatory infiltrate, indicative of mild colitis, as illustrated in (Fig. 13 and Fig. 14). The results further confirmed that dox-proc exhibited an enhanced therapeutic effect in the treatment of colitis.

Group I (Control)

The histopathological figures of the mucosa of colon showed normal epithelial mucosa, normal cellular lamina propria, simple tubular mucous glands and normal submucosa (Fig.9).

Group II (AA)

The histopathological figures revealed severe reactive chronic colitis that characterized by inflammation with congestion of mucosa the inflammatory infiltrates comprised mainly of plasma cells, lymphocytes and macrophages while the submucosa showed marked aggregation with proliferation of lymphocytes, absence of granulomatous lesions and absence of ulcers (Fig.10).

Group III (dox-proc)

The Figures of colon showed little patch of marked hypoplasia of tubular glands with marked reduce secretion and atrophy, little fibroplasia of lamina propria fibrous tissue with marked dilation of other glands with atrophy of lining cells. The surfaces of colon lining cells showed mucoid degeneration, mucosa of colon showed normal appearance with lining cells of tubular gland and normal secretory activities (Fig.11).

Group IV (SULF)

The figures of colon showed marked hypoplasia of tubular glands with marked reduce secretion and atrophy, insignificant

fibroplasia of lamina propria fibrous tissue with noticeable dilation of other glands with atrophy of lining cells. The surfaces lining cells of colon lining cells showed mucoid degeneration. other figures of mucosa of colon showed normal appearance with lining cells of tubular gland and normal secretory activities (Fig. 12).

Group V (doxycycline)

The histopathological Figures of the colon revealed mild colitis that are characterized by mild necrosis with sloughing of epithelial mucosa, mild cellulitis of lamina propria, degeneration with necrosis and little atrophy of mucous glands. The submucosa showed mild infiltration of leukocytes (Fig. 13).

Group VI (procaine)

Show mild colitis in which mild necrosis with sloughing of epithelial mucosa, acute cellulitis of lamina propria, degeneration with necrosis and atrophy of mucous glands (Fig. 14).

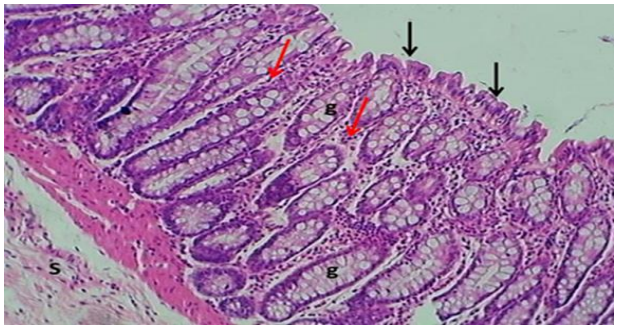

Figure (9): The colon segment (control) exhibits normal epithelial mucosa (black arrows), intact cellular lamina propria (red arrows), simple tubular mucous glands (g) and normal submucosa (S). Hematoxylin and Eosin, 100x magnification.

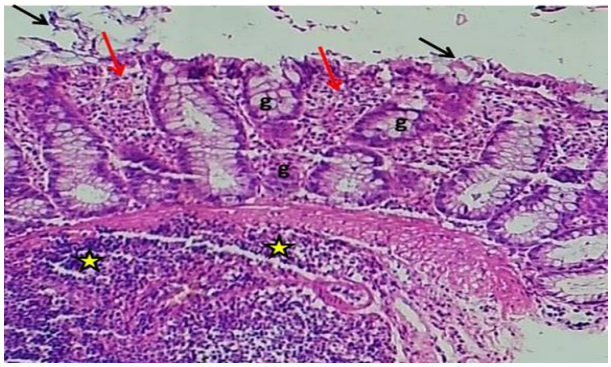

Figure (10): The colon segment (AA) group (severe colitis) exhibits pronounced necrosis accompanied by sloughing of the epithelial mucosa (black arrows), severe cellulitis in the lamina propria (red arrows), degeneration with necrosis and atrophy of mucous glands (g), and significant aggregation of leukocytes inside the submucosa (asterisks). Hematoxylin and Eosin, 100x magnification.

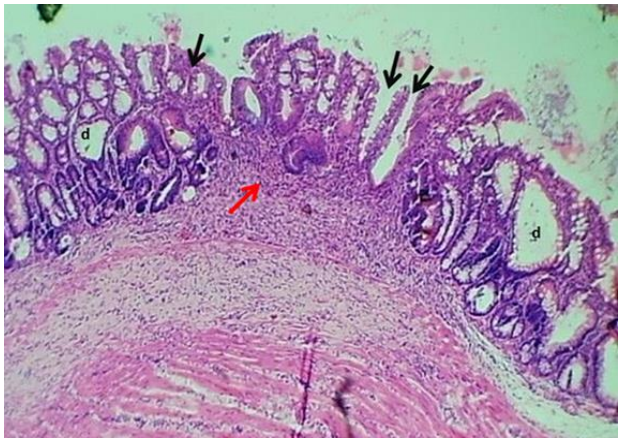

Figure (11): section of colon mucosa (dox-proc) group shows marked hypoplasia of tubular glands with marked reduce secretion and atrophy (Black arrows) little fibroplasia of propria fibrous tissue (Red arrows) with marked dilation of other glands with atrophy of lining cells (d). Hematoxylin and Eosin, 40x magnification.

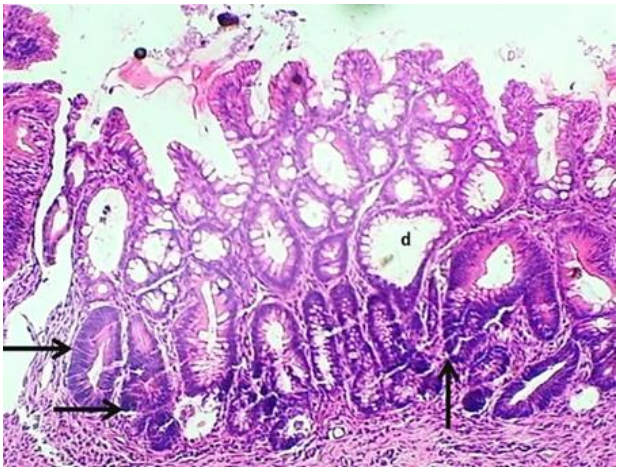

Figure (12): section of colon mucosa (SULF) shows deepest layer of glands showed hyperplasia (Black arrows) with dilation of other glands with atrophy of lining cells (d). Hematoxylin and Eosin, 100x magnification.

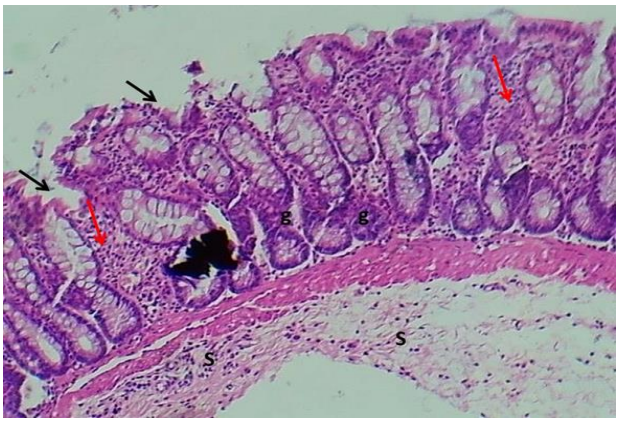

Figure (13): The colon segment (doxycycline) group (mild colitis) exhibits minor necrosis accompanied by sloughing of the epithelial mucosa (black arrows), slight cellulitis in the lamina propria (red arrows), degeneration with necrosis and atrophy of mucous glands (g), and mild leukocyte infiltration inside the submucosa (S). Hematoxylin and Eosin, 100x magnification.

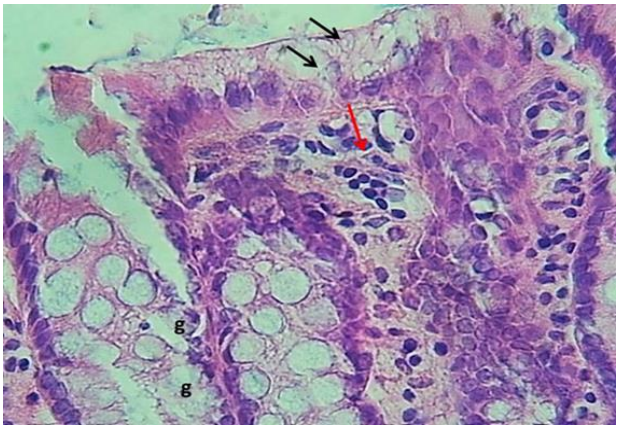

Figure (14): The colon segment (procaine) group (mild colitis) exhibits minor degeneration accompanied by necrosis and sloughing of the epithelial mucosa (black arrows), slight cellulitis of the lamina propria (red arrows), and degeneration with necrosis and atrophy of the mucous glands (g). Hematoxylin and Eosin, 400x magnification.

Discussion

The results of our integrated study underline the successful design and synthesis of a colon-targeted mutual prodrug of

doxycycline and procaine. In silico ADME evaluations predicted poor intestinal absorption due to increased molecular weight, pronounced hydrophilicity (log P < 0), and a high TPSA (235.88 Å2), all critical parameters that reduce passive uptake across the intestinal epithelium. These characteristics ensure minimal systemic absorption and favor delivery to the colon. Computational molecular docking to the azoreductase enzyme exhibited a good binding affinity compared to sulfasalazine, the clinical standard for colonic prodrug activation.

Experimental studies corroborated these predictions: the compound's log P equal to (–1.65), confirmed its hydrophilic nature, and stability assays established a low rate of degradation in gastric (acidic) conditions, safeguarding the prodrug during gastrointestinal transit. Stability in basic media was also satisfactory, supporting its integrity prior to colonic activation.

The bioactivation potential was demonstrated by fecal hydrolysis in vitro, revealing that the prodrug undergoes efficient cleavage (81%) in the presence of bacterial azoreductase enzyme a crucial step for therapeutic effect in ulcerative colitis. In vivo, treated rats exhibited significant symptom improvement as assessed by clinical activity scoring and histopathological analysis, which revealed substantial mucosal regeneration and reduction of inflammatory signs.

Taken together, these multidimensional results validate the mutual prodrug design, in silico strategy, and biological efficacy for colonic drug delivery. The observed harmony between computational prediction, chemical characterization, and in vivo therapeutic response supports further development toward clinical application.

Future Work

To advance the scope and impact of this promising prodrug, future research should address the following:

- **Molecular Mechanism Studies:** Examine anti-inflammatory pathways and molecular markers, such as interleukin-6 (IL-6) and tumor necrosis factor-alpha (TNF-α), and others. To elucidate the pharmacodynamic mechanisms.
- **Antioxidant and Anticancer Assessment:** Evaluate antioxidant capacity and anticancer properties to expand potential indications.
- **Comprehensive Pharmacokinetics:** Include in vivo absorption, metabolism, and elimination studies to confirm colon-selectivity and systemic safety.
- **Formulation Optimization:** Develop oral delivery systems, such as coated tablets or capsules, to maximize colonic targeting and patient compliance.
- **Comparative Efficacy:** Benchmark therapeutic effects against established treatments (e.g., sulfasalazine, mesalazine) in larger animal cohorts or diverse models of colitis.

These steps will strengthen the evidence base, clarify the mechanisms of action, and support eventual translation into clinical trials.

Conclusion

This study addressed the need for targeted ulcerative colitis therapy by designing a colon-specific mutual prodrug of doxycycline and procaine. Key findings showed that unfavorable intestinal absorption properties (high molecular weight, low log P, and high TPSA) and high enzymatic hydrolysis by colonic azoreductase achieved effective site-specific activation, leading to significant clinical and histological improvements in treated rats. The combined use of in-silico and experimental approaches validated the prodrug's stability and selectivity for colonic delivery.

In conclusion, this mutual prodrug strategy offers a promising platform for targeted ulcerative colitis therapy and warrants further mechanistic and translational study.

Disclosure statement

- **Ethics approval and consent to participate:** The Institutional Ethical Committee of the college of Pharmacy at al- Mustansiriyah University reviewed and approved the protocol.
- **Author's contribution:** All authors contributed equally to this research.
- **Conflicts of interest:** The authors report no conflicts of interest.
- **Funding:** This research has been self-funded, as it did not receive any specific grant from external sources.
- **Acknowledgement:** The authors would like to thank Mustansiriyah University Baghdad- Iraq for its support in the present work.

Open Access

References

1] Diez-Martin E, Hernandez-Suarez L, Muñoz-Villafranca C, Martin-Souto L, Astigarraga E, Ramirez-Garcia A, Barreda-Gómez G. Inflammatory Bowel Disease: A Comprehensive Analysis of Molecular Bases, Predictive Biomarkers, Diagnostic Methods, and Therapeutic Options. International Journal of Molecular Sciences. 2024; 25(13):7062. https://doi.org/10.3390/ijms25137062

2] Suman S. Enteric Nervous System Alterations in Inflammatory Bowel Disease: Perspectives and Implications. Gastrointestinal Disorders. 2024; 6(2):368-379. https://doi.org/10.3390/gidisord6020025

3] Zhao Z, Liu X, Zhang R, Ke R, Zhang S, Chen Y. Intestinal Barrier in Inflammatory Bowel Disease: Mechanisms and Treatment. J Transl Gastroenterol. 2025;3(2):62-73. https://doi:10.14218/JTG.2024.00038.

4] Burgos-Molina AM, Téllez Santana T, Redondo M, Bravo Romero MJ. The Crucial Role of Inflammation and the Immune System in Colorectal Cancer Carcinogenesis: A Comprehensive Perspective. International Journal of Molecular Sciences. 2024; 25(11):6188. https://doi.org/10.3390/ijms25116188

5] Jaroenlapnopparat A, Bhatia K, Coban S. Inflammation and Gastric Cancer. Diseases. 2022 Jun 22;10(3):35. https://doi: 10.3390/diseases10030035

6] Ramaite FT, Nkadimeng SM. Targeting inflammatory pathways in hepatocellular carcinoma: recent developments. Discov Onc 2025; 16: 1174. https://doi.org/10.1007/s12672-025-03035-8

7] Liu YY, Ohashi Y, Ushijima T. How chronic inflammation fuels carcinogenesis as an environmental epimutagen. Discov Onc. 2025; 16: 1150. https://doi.org/10.1007/s12672-025-02971-9

8] Nishida A, Andoh A. The Role of Inflammation in Cancer: Mechanisms of Tumor Initiation, Progression, and Metastasis. Cells. 2025; 14(7):488. https://doi.org/10.3390/cells14070488

9] Olivia M D, Aaron J S, Diane N K, Annika R S. Chronic Inflammation to Cancer: The Impact of Oxidative Stress on DNA Methylation. Front. Biosci. (Landmark Ed).2025; 30(3):26142. https://doi.org/10.31083/FBL26142

10] Strupp C, Corvaro M, Cohen SM, Corton JC, Ogawa K, Richert L, Jacobs MN. Increased Cell Proliferation as a Key Event in Chemical Carcinogenesis: Application in an Integrated Approach for the Testing and Assessment of Non-Genotoxic Carcinogenesis. International Journal of Molecular Sciences. 2023; 24(17):13246. https://doi.org/10.3390/ijms241713246

11] Xiaotong W, Yunqiu S, Yan C, Shuang Y.Inflammation-induced cellular changes: Genetic mutations, oncogene impact, and novel glycoprotein biomarkers. Advances in Biomarker Sciences and Technology. 2024; 6:91-104. https://doi.org/10.1016/j.abst.2024.06.002.

12] Vaidya H, Jelinek J, Issa J-PJ. DNA Methylation, Aging, and Cancer. Epigenomes. 2025; 9(2):18. https://doi.org/10.3390/epigenomes9020018

13] Li Y, Tian X, Luo J. Molecular mechanisms of aging and anti-aging strategies. Cell Commun Signal. 2024; 22. https://doi.org/10.1186/s12964-024-01663-1

14] Hong Y, Boiti A, Vallone D, Foulkes NS. Reactive Oxygen Species Signaling and Oxidative Stress: Transcriptional Regulation and Evolution. Antioxidants. 2024; 13(3):312. https://doi.org/10.3390/antiox13030312

15] Dai Y, Guo Y, Tang W. Reactive oxygen species-scavenging nanomaterials for the prevention and treatment of age-related diseases. J Nanobiotechnol.2024; 22: 252. https://doi.org/10.1186/s12951-024-02501-9

16] Giovanni C, Serena P, Nicolas B. Gut microbiota in inflammation and colorectal cancer: A potential Toolbox for Clinicians,Best Practice & Research Clinical Gastroenterology. Elsevier Ltd; 2024. https://doi.org/10.1016/j.bpg.2024.101942.

17] Xu Y, Gao Z, Liu J, Yang Q, Xu S. Role of gut microbiome in suppression of cancers. Gut Microbes. 2025 Dec; 17(1): 2495183. https://doi: 10.1080/19490976.2025.2495183.

18] Shayista H, Nagendra Prasad MN, Niranjan Raj S., Ashwini P, Lakshmi S, Ranjini HK, Manju K, Ravikumara, Raghuraj S C, Olga Y K, Olga V P, Syed B. Complexity of antibiotic resistance and its impact on gut microbiota dynamics. Engineering Microbiology. 2025; 5(1): 100187. https://doi.org/10.1016/j.engmic.2024.100187.

19] Chen C, Su Q, Zi M, Hua X, Zhang Z. Harnessing gut microbiota for colorectal cancer therapy: from clinical insights to therapeutic innovations. npj Biofilms Microbiomes. 2025; 11:190. https://doi.org/10.1038/s41522-025-00818-3

20] Xuewei Y, Anqi W, Wenting L, Yiwen X, Xinyi D, Yue Z, Kewei T, Xiaoling X. The Role of Intestinal Flora in Anti-Tumor Antibiotic Therapy. Front. Biosci. (Landmark Ed). 2022; 27(10): 281. https://doi.org/10.31083/j.fbl2710281

21] Zhuang J, Wu Y, Chu J, Qu Z, Wu X, Han S. Interaction between gut microbiota and T cell immunity in colorectal cancer,Autoimmunity Reviews. 2025; 24(6):103807. https://doi.org/10.1016/j.autrev.2025.103807.

22] Lei W, Zhou K, Lei Y, Li Q, Zhu H. Gut microbiota shapes cancer immunotherapy responses. npj Biofilms Microbiomes. 2025; 11(143). https://doi.org/10.1038/s41522-025-00786-8

23] Zhang PF, Xie D. Targeting the gut microbiota to enhance the antitumor efficacy and attenuate the toxicity of CAR-T cell therapy: a new hope? Front Immunol. 2024 Mar 15;15:1362133. https://doi:10.3389/fimmu.2024.1362133.

24] Lily K, John F C, Jack P G.Exploiting the gut microbiome for brain tumour treatment.Trends in Molecular Medicine. 2025; 31(3): 213-223. https://doi.org/10.1016/j.molmed.2024.08.008.

25] Besselink N, Keijer J, Vermeulen C. The genome-wide mutational consequences of DNA hypomethylation. Sci Rep. 2023; 13. https://doi.org/10.1038/s41598-023-33932-3

26] Laura E M, Alessia F, Atheer A, Mine O, Simon G, Abdul W B. Colonic drug delivery: Formulating the next generation of colon-targeted therapeutics. Journal of Controlled Release. 2023 ; 353:1107-1126.https://doi.org/10.1016/j.jconrel.2022.12.029.

27] Ivan K, Michaela D, Dani D, Bożena Futoma-K, Márió G, Lamiaa A. Al-M, Mohamed Abd El-S. Advances in gut microbiota functions in inflammatory bowel disease: Dysbiosis, management, cytotoxicity assessment, and therapeutic perspectives.Computational and Structural Biotechnology Journal. 2025; 27: 851-868. https://doi.org/10.1016/j.csbj.2025.02.026.

28] Laffusa A, Burti C, Viganò C, Poggi F, Grieco L, Occhipinti V, Greco S, Orlando S. Inflammatory Bowel Disease: Understanding Therapeutic Effects of Distinct Molecular Inhibitors as the Key to Current and Future Advanced Therapeutic Strategies. Biomedicines. 2025; 13(11):2667. https://doi.org/10.3390/biomedicines13112667

29] Hammoodi S, Hasan I S, Sedqi M Y F. Mutual prodrugs for colon targeting: A review. Journal of Medicinal and Pharmaceutical Chemistry Research. 2022; 4(12): 1251-1265.

30] Sheikh NK, Dua A. Procaine. [Updated 2023 May 8]. In: StatPearls [Internet]. Treasure Island (FL): StatPearls Publishing; 2025 Jan-. https://www.ncbi.nlm.nih.gov/books/NBK551556/

31] Song W, Zhang H, Li X, Yu C, Zhou Y, Li Y, Chen B. Delayed lethal central nervous system toxicity induced by a low-dose intrathecal administration of bupivacaine: case report. Frontiers in Anesthesiology. 2023; 2. DOI=10.3389/fanes.2023.1298806

32] Gradinaru D, Ungurianu A, Margina D, Moreno-Villanueva M, Bürkle A. Procaine-The Controversial Geroprotector Candidate: New Insights Regarding Its Molecular and Cellular Effects. Oxid Med Cell Longev. 2021 Jul 31:3617042. https:// doi: 10.1155/2021/3617042.

33] Jeffrey C P, Eric G, Nora D G, Brandon D. Tetracyclines, the old and the new: A narrative review. CMI Communications. 2025; 2(1). https://doi.org/10.1016/j.cmicom.2025.105059.

34] Radić M, Belančić A, Đogaš H, Vučković M, Gelemanović A, Faour A, Vlak I, Radić J. Tetracyclines in Rheumatoid Arthritis: Dual Anti-Inflammatory and Immunomodulatory Roles, Effectiveness, and Safety Insights. Antibiotics. 2025; 14(1):65. https://doi.org/10.3390/antibiotics14010065

35] Fan S, Zhao Y, Yao Y. Oral colon-targeted pH-responsive polymeric nanoparticles loading naringin for enhanced

ulcerative colitis therapy. J Transl Med. 2024; 22: 878. https://doi.org/10.1186/s12967-024-05662-1

36] Thuiny HT, Fahad TA, Ali AA. Preparation, analytical Studies and application of a New Azodye Derived from Pharmaceutical Materials (Procaine Hydrochloride & Salicylic acid). InJournal of Physics: Conference Series 2021 Nov 1 (Vol. 2063, No. 1, p. 012024). IOP Publishing.

37] Tabarak M, Hind H. Normal and reverse flow injection-spectrophotometric determination of doxycycline hyclate in bulk and pharmaceutical samples. Baghdad Science Journal. 2025; 22(8). https://doi.org/10.21123/2411-7986.5016

38] Farooq M H, Ayad K K, Shakir M A. In Silico Molecular Modelling and Dynamic Simulations, ADME Parameters Predictions of new Naproxen Analogues Containing 1,3,4-Oxadiazole as Anti-inflammatory Agents. Turkish Comp Theo Chem (TC&TC). 2025; 9(4): 15-28.

39] Muhammad T I, Adamu U, Bello AU, Bello AS, Yusuf I. Molecular Modelling, Docking and Pharmacokinetic Studies of N-Arylidenequinoline-3-Carbohydrazides Analogs as Novel β-Glucuronidase Inhibitors. J. Mex. Chem. Soc. 2020; 64(1). https://doi.org/10.29356/jmcs.v64i1.1025

40] Daria K, Małgorzata J, Małgorzata D, BeataMorak-M. Study of the Lipophilicity and ADMET Parameters of New Anticancer Diquinothiazines with Pharmacophore Substituents. Pharmaceuticals. 2024; 17(725). https://doi.org/10.3390/ph17060725

41] Agu PC, Afiukwa CA, Orji OU, Ezeh EM, Ofoke IH, Ogbu CO, Ugwuja EI,Aja P M. Molecular docking as a tool for the discovery of molecular targets of nutraceuticals in diseases management. Sci Rep. 2023; 13: 13398. https://doi.org/10.1038/s41598-023-40160-2

42] Agüero FA, Maglioco A, Valacco MP, Juárez Valdez AY, Roldán E, Paulino M, Fuchs AG. First In Silico Study of Two Echinococcus granulosus Glyceraldehyde-3-Phosphate Dehydrogenase Isoenzymes Recognized by Liver Cystic Echinococcosis Human Sera. International Journal of Molecular Sciences. 2025; 26(21):10622. https://doi.org/10.3390/ijms262110622

43] Meeqaat H AL-T, Samer AH, Zeyad K O. New Isatin-Thiazolidinone Hybrids Targeting Melanoma: Rational Design, Synthesis, And Molecular Docking Supported By Pharmacokinetic And Toxicological Predictions. IJEES. 2025; 15 (5): 307-317. https://doi.org/10.31407/ijees15.4

44] Jerome E, Stefano F. WaterKit: Thermodynamic Profiling of Protein Hydration Sites.Journal of Chemical Theory and Computation. 2023; 19 (9): 2535-2556. DOI: 10.1021/acs.jctc.2c01087

45] Nisarg R, Priyanka S, Rukmankesh M, Anu M. Identification of natural compound inhibitors for substrate-binding site of MTHFD2 enzyme: Insights from structure-based drug design and biomolecular simulations. Chemical Physics Impact. 2025; 10: 100809. https://doi.org/10.1016/j.chphi.2024.100809.

46] Coutinho AL, Cristofoletti R, Wu F, Al Shoyaib A, Dressman J, Polli J E. Relative Performance of Volume of Distribution Prediction Methods for Lipophilic Drugs with Uncertainty in LogP Value. Pharm Res. 2024; 41: 1121–1138. https://doi.org/10.1007/s11095-024-03703-4

47] Tang S, Wang W, Wang Y, Gao Y, Dai K, Zhang W, Wu X, Yuan X, Jin C, Zan X, Zhu L, Geng W. Sustained release of 5-aminosalicylic acid from azoreductase-responsive polymeric prodrugs for prolonged colon-targeted colitis therapy. J Nanobiotechnol. 2024; 22(468). https://doi.org/10.1186/s12951-024-02724-w

48] Karbasi AB, Barfuss JD, Morgan TC, Collins D, Costenbader DA, Dennis DG, Hinman A, Ko K, Messina C, Nguyen KC, Schugar RC, Stein KA, Williams BB, Xu H, Annes JP, Smith M. Sol-moiety: Discovery of a water-soluble prodrug technology for enhanced oral bioavailability of insoluble therapeutics. Nat Commun. 2024 Oct 1;15(1):8487. doi: 10.1038/s41467-024-52793-6.

49] Amrita N, Sudip KM, Mohmmed R, Santosh. Formulation, Development and Physicochemical Characterization of Diclofenac Topical Emulgel. Egyptian Journal of Chemistry. 2021; 64(3). DOI: 10.21608/ejchem.2021.58467.3259

50] Hu Q, Yammani RD, Brown-Harding H, Soto-Pantoja DR, Poole LB, Lukesh JC 3rd. Mitigation of doxorubicin-induced cardiotoxicity with an H2O2-Activated, H2S-Donating hybrid prodrug. Redox Biol. 2022 Jul;53:102338. doi: 10.1016/j.redox.2022.102338

51] Mahdy RNE, Nader M., Helal MG. Protective effect of Dulaglutide, a GLP1 agonist, on acetic acid-induced ulcerative colitis in rats: involvement of GLP-1, TFF-3, and TGF-β/PI3K/NF-κB signaling pathway. Naunyn-Schmiedeberg's Arch Pharmacol. 2025; 398: 5611–5628. https://doi.org/10.1007/s00210-024-03631-5

52] Hadeer A, Abd-Allah A M, Wael M G, Emad W G, Mohamed F Abou E, Alaa A, Zizy I E, Doaa H A. Chlorella vulgaris Effectively Attenuates Acetic acid-induced Colitis in Rats by Inhibiting NF-κB, and Caspase-3, While Activating IL-10 Expression. Egypt. J. Vet. Sci. pp. 1-21. https://doi.org/10.21608/ejvs.2024.289158.2084

53] Zabihi M, Aminalroayaei F, Motaghi-Dastnaei E, Dara T. Impact of Eugenol on Acetic acid-induced Colitis in Rats. AdvPharmacol Ther J. 2023;3(3): 114-122. https://doi.org/10.18502/aptj.v3i3.14415

54] Babalola WO, Ofusori DA, Awoniran P, Falana BA. Aloe vera gel attenuates acetic acid-induced ulcerative colitis in adult male Wistar rats. Toxicol Rep. 2022 Apr 1; 9:640-646. https://doi.org/10.1016/j.toxrep.2022.03.048

55] Otu-Boakye SA, Yeboah KO, Boakye-Gyasi E, Oppong-Kyekyeku J, Okyere PD, Osafo N. Acetic acid-induced colitis modulating potential of total crude alkaloidal extract of Picralima nitida seeds in rats. Immun Inflamm Dis. 2023 May;11(5): e855. https://doi.org/10.1002/iid3.855

56] Dawood JO, Abu-Raghif A. Labetalol Ameliorates Experimental Colitis in Rat Possibly Through its Effect on Proinflammatory Mediators and Oxidative Stress. Clin Lab. 2024 Feb 1;70(2). https://doi.org/10.7754/clin.lab.2023.230659

57] Mahzouni, P., Nasr Esfahani, S., Minaiyan, M., Asghari, G., Saeidi, M. Anti-Inflammatory Effect of Curcuma Longa on Ulcerative Colitis Caused via AcOH in Rats. Journal of Medicinal and Chemical Sciences, 2023; 6(8): 1915-1924. https://doi.org/10.26655/JMCHEMSCI.2023.8.20

58] Derardja I, Rebai R, Toumi ME, Kebaili FF, & Boudah A. Identification of New Potential Cyclooxygenase-2 Inhibitors Using Structure-Based Virtual Screening, Molecular Dynamics and Pharmacokinetic Modelling. Biology and Life Sciences Forum. 2024; 35(1): 6. https://doi.org/10.3390/blsf2024035006

59] Hiron S D, Maisha M M, Md N I, Partha B, Debasree S O, Arafat H, Rubaet S E, Md M I T, Mimi G, Md NH, Biswajit B, Samir KS.Bioactive small compounds effectively inhibit ChREBP overexpression to treat NAFLD and T2DM: A

computational drug development approach. Heliyon. 2025; 11(4). https://doi.org/10.1016/j.heliyon.2025.e42477.